**REM WORKING PAPER SERIES**

# Hospital Admission Rates in São Paulo, Brazil - Lee-Carter model vs. neural networks

**Rodolfo Monfilier Peres, Onofre Alves Simões**

**REM Working Paper 0349-2024**

October 2024

**REM – Research in Economics and Mathematics**
Rua Miguel Lúpi 20,
1249-078 Lisboa,
Portugal

ISSN 2184-108X

**REM – Research in Economics and Mathematics**

Rua Miguel Lupi, 20
1249-078 LISBOA
Portugal

Telephone: +351 - 213 925 912
E-mail: rem@iseg.ulisboa.pt

https://rem.rc.iseg.ulisboa.pt/

https://twitter.com/ResearchRem

https://www.linkedin.com/company/researchrem/

https://www.facebook.com/researchrem/

Hospital Admission Rates in São Paulo, Brazil - Lee-Carter model vs. neural networks

Rodolfo Monfilier Peres[1]
Onofre Alves Simões[2,3]

Abstract
In Brazil, hospital admissions account for nearly 50% of the total cost of health insurance claims, while representing only 1% of total medical procedures. Therefore, modeling hospital admissions is useful for insurers to evaluate costs in order to maintain their solvency. This article analyzes the use of the Lee-Carter model to predict hospital admissions in the state of São Paulo, Brazil, and contrasts it with the Long Short Term Memory (LSTM) neural network. The results showed that the two approaches have similar performance. This was not a disappointing result, on the contrary: from now on, future work can further test whether LSTM models are able to give a better result than Lee-Carter, for example by working with longer data sequences or by adapting the models.

Keywords: Hospital Admissions; Lee-Carter; Neural Networks; LSTM; Brazil

1. Introduction
The Lee-Carter model (Lee & Carter, 1992) remains a foundation model for mortality forecasting in several developed countries, such as Denmark, Sweden, Canada, and Italy (Rabbi & Mazzuco, 2020; Steeghs, 2020; Kjærgaard & Bergeron-Boucher, 2022). While its primary application has been in mortality forecasting and there are few uses outside this area (Frees, 2006), some extensions have emerged, including its use in health insurance (Lee & Miller, 2002) and in predicting hospital admission rates (Rodrigues et al., 2013). In recent years, there has been a significant shift toward leveraging neural networks for mortality modeling, with several studies showcasing their efficacy (Nigri et al., 2019; Nigri et al., 2021; Hainaut, 2018; Deprez et al., 2017; Richman & Wüthrich, 2018; Perla et al., 2021). Notably, the integration of neural networks with the Lee-Carter model represents a novel avenue within the actuarial field, with initial explorations emerging in 2018 (Hainaut, 2018). Given the profound impact of adverse events on health insurers' liabilities and financial sustainability, further research in this area is imperative, particularly in developing more accurate models for forecasting hospital admissions.
In Brazil, hospital admissions represent almost 50% of the total claim cost of health insurance companies while representing only 1% of the total medical procedures (Cechin & Lara, 2020). Given that, modeling hospital admissions is extremely useful for health insurers to assess their claim costs over time. Adverse events can seriously strain their liabilities, and actuaries should be well prepared to assess that to keep the financial sustainability of the companies, given their pivotal social and economic role. The main purpose of our paper is to add a contribution to the set of possible applications of neural network techniques in the actuarial science field, by dealing with this problem. For that,

[1] ISEG, rodolfo.peres@aln.iseg.ulisboa.pt
[2] ISEG-UL, onofre@iseg.ulisboa.pt
[3] REM, CEMAPRE
This work was supported by FCT (*Fundação para a Ciência e a Tecnologia*) [grant number UIDB/05069/2020].

we model hospital admissions rates in São Paulo, Brazil, following up the seminal work by Rodrigues et al. (2013). The idea is to revisit the problem of modelling the admission rates, in light of the recent studies that combine the Lee-Carter model (Lee & Carter, 1992) with neural networks, and to contrast the two approaches, in order to determine if the neural networks can provide improvements over what has been done before.

In 1992 (Lee & Carter, 1992) proposed a new model for estimating mortality rates. It became widely spread and the leading statistical model for mortality forecasting (Wilmoth, 1996, Deaton & Paxson, 2004, Hollmann et al., 2000, Tuljapurkar et al., 2000). Lee and Carter seek to summarize an age-period surface of log-mortality rates in terms of an average age profile of mortality, mortality changes over time, and how much each age group changes when mortality changes. However, its popularity and simplicity did not prevent the model from being criticized, mostly because it assumes that all information about future mortality is contained in the past observed data, not including important covariates such as tobacco use, alcohol consumption or comorbidity (Girosi & King, 2008). Moreover, exogenous shocks such as new medical technologies, economic crises, pandemics, etc. are ignored (Gutterman & Vanderhoof, 1998).

In recent years, most healthcare systems are going through reforms, attempting to control the raising costs. Generally, most reforms focus on strengthening primary care, adopting mechanisms for supply-induced demand, new forms of care (i.e. home care and long-term care), and promoting changes to achieve a better lifestyle. In light of these reforms, several studies have focused on forecasting health care expenditures and utilization, assuming that costs remain constant and are only affected by the size and age structure of the population, i.e., the pure demographic effect (Tate et al., 2005; Lindberg & McCarthy, 2021). The main caveat is that they can only be used in short-period analyses since changes in utilization patterns are not incorporated. Other (non-traditional) methods have tried to forecast healthcare expenditure based on time series analyses (Tate et al., 2005), or on the use of panel data including other covariates such as income and education (Xu et al., 2011; European Commission, 2013).

Research contributions that combine the use of the Lee-Carter model and neural networks in the demographic field of study have been growing recently. Deprez et al. (2017) used machine learning algorithms to assess the goodness of fit of standard mortality models. They analyze how a standard mortality model could be improved based on feature components of an individual, such as age. This work was further extended by (Levantesi & Pizzorusso, 2019), who used machine learning algorithms to calibrate a parameter that was applied to mortality rates fitted by standard mortality models.

Although both papers applied machine learning techniques in the field of mortality modeling, none of them have specifically used neural networks. The use of neural networks to predict mortality rates started with (Hainaut, 2018), by proposing a neural network that detects the non-linearities in the structure of the log-forces of mortality. In the same year, Richman & Wüthrich (2018) proposed a Lee-Carter approach for multiple populations, where the parameters were estimated by neural networks. Nigri et al. (2019) use the Long Short-Term Memory (LSTM) neural network to improve the accuracy of predictions of the general level of mortality given by the Lee-Carter model. Nigri et al. (2021) consider an LSTM model to predict mortality and lifespan in five developed countries. Comparing the results with standard models, they conclude that their predictions provide a more accurate portrait. In another recent study, Perla et al. (2021) tested several neural networks to simultaneously predict mortality in different countries, showing that great accuracy can be achieved in a large-scale prediction.

## 2. Methodology and Data

### 2.1 Methodology

The Lee-Carter model (Lee & Carter, 1992), developed for mortality forecasting is

$$\log(u_{x,t}) = a_x + b_x k_t + e_{x,t} \qquad (1)$$

where $u_{x,t}$ is the death rate for age *x* in year *t*, $a_x$ is the average log of mortality at age $x$, $b_x$ is the rate of change of the log mortality with time at age $x$, $k_t$ is the general level of mortality for calendar year $t$, and $e_{x,t}$ is the residual term at age $x$ and time $t$. It is a two-fold model. Firstly, parameters $a_x$, $b_x$ and $k_t$ need to be estimated. Secondly, the fitted $k_t$ values are modeled as an ARIMA(*p, q, d*) process.

Since we use (1) to model hospital admission rates, the variables assume a new interpretation: $u_{x,t}$ is now the hospitalization rate for age *x* in year *t*, $a_x$ is the average log of hospitalization at age $x$, $b_x$ is the rate of change of the log hospitalization with time at age $x$, $k_t$ is the general level of hospitalization for calendar year $t$ and $e_{x,t}$ is the residual term at age $x$ and time $t$. We will obtain the parameters $a_x$ and $b_x$ and we will estimate the $k_t$ trend by an $ARIMA(p,d,q)$ model, divided by gender. We follow Nigri et al. (2019) and estimate the $ARIMA(p,d,q)$ by using the *auto.arima* function from the R package *forecast* (Hyndman & Khandakar, 2008; Hyndman et al., 2022). This package applies the Hyndman-Khandakar algorithm (Hyndman & Khandakar, 2008) to automatically select the best $ARIMA(p,d,q)$ model for a given time series. Because the $k_t$ series presents monthly seasonality, a SARIMA model was used for the prediction. The series was split in two, one for training the model with the first 131 data points and another one for testing the model with the final 12 months of data. To complete the experiment, the following 12 months of $k_t$ were predicted.

Neural networks are mathematical models based on the biological neural network structures of the brain (Minsky & Seymour, 2017; McCulloch & Pitts, 1943; Wiener, 1948). The general neural network model is formed by an input layer, one or several hidden layers, and an output layer and each of them is composed of several neurons (Nigri et al., 2019). In the recurrent neural networks (RNN) structure, the information moves cyclically in the network using additional synapses. They are a special case of neural networks where the objective is to predict future steps in a sequence of observations (Namini & Namin, 2018). The LSTM models are RNNs whose architecture is built in such a way that it allows for considering the relationships between the data of the sequence, even if it is long. Hence, LSTMs acquire both long and short-term memory (Hochreiter & Schmidhuber, 1997; Gers, et al., 2000; Nigri et al., 2019). In our work the model was implemented in R, using the packages *Keras* (Chollet, 2015) and *TensorFlow* (Abadi, 2015). A major aspect is that the neural network demands great data preparation before the model can be fit (Brownlee, 2018).

To choose the model structure, the first task is to determine the number of neurons and layers. Neural network architecture typically relies on human knowledge and trial and error (Dong et al., 2021; Hu et al. (2021). Neural architecture search (NAS) has been proposed to automatically search the best architecture for neural networks, but currently algorithms suffer from computational cost (Jin et al., 2019). In the end, we decided to have a simple neural network model that could be easily contrasted with the ARIMA model, see Figure 1.

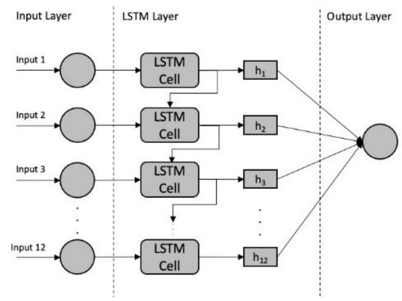


Figure 1. LSTM architecture used in this work

The input layer has 12 neurons because each neuron represents one data point of the input sequence. Regarding the hidden layer, problems that require two or more hidden layers are not commonly seen (Heaton, 2005), since training can be too difficult, due to the increase in the number of parameters, overall complexity and time required to execute the model (Uzair & Jamil, 2020). Considering the complexities that adding hidden layers imposes and since in this work we are dealing with only one predictor, we chose to have only one hidden layer. The output layer is composed of a single neuron that outputs a sequence of 12 predictions. Even though the used architecture seems to be simple, it has 685 adjustable parameters. The learning rate is a parameter that should be empirically chosen and is one of the most important parameters to adjust in a neural network architecture (Bengio, 2012). A default value of 0.01 typically works for default neural networks but other values should be tested as well (Bengio, 2012). Values tested are usually small e.g., a learning rate within the set $\{0.1, 0.01, 10^{-3}, 10^{-4}, 10^{-5}\}$ (Goodfellow et al., 2016, p. 436). Despite of only choosing a fixed value for the learning rate, Wang et al. (2019) have shown that using a learning rate decay can provide benefits for training neural networks. In this approach, the learning rate starts with a given value that decays by a factor during the iterations. In the end, we tested four learning rates and five decay values, per gender, to find the two combinations that minimize the cost function.

4.2 Data

Hospitalization data from the State of São Paulo was gathered from *Serviço de Informações Hospitalares do Sistema Único de Saúde* (Hospital Information System of the Unified Health System - SIH/SUS) and the data from the population resident in the State of São Paulo was gathered from *Pesquisa Nacional por Amostragem de Domicílios do Instituto Brasileiro de Geografia e Estatística* (National Sample Household Survey of the Brazilian Institute of Geography and Statistics - PNAD/IBGE), both from Jan/2008 until Nov/2019. The hospitalization data encompasses all private and public hospital admissions. These two sources of data supplied full data used in our study.

The hospitalization data is monthly available while the data from the population resident in the state of São Paulo is only available at the end of the year. This annual data was transformed into monthly data, assuming that each observed annual increase/decrease in the resident population occurred uniformly during the year (United Nations, 1952). The choice of gathering data from 2008 onwards was made because this is the first year when the dates of hospital admissions started to be registered. Also, Nov/2019 was chosen as the final month because of COVID-19 pandemic in Brazil. The first COVID infection was reported in Feb/2020 by Brazilian authorities but we can see great distortions in data from Dez/19 onwards.

The data provided by SIH/SUS is available in 18 age groups: < 1 year old, 1-4 years old, …, 75-79 years old, 80+ years old. The data provided by PNAD/IBGE is in 15 age groups: 0-4 years old, …, 70+ years old. To overcome this mismatch, the data from SIH/SUS was adjusted to the same standard of the PNAD/IBGE data. The data from SIH/SUS was put in the same standard as the data of PNAD/IBGE by summing the SIH/SUS data into the PNAD/IBGE age group standard.

Figures 2 and 3 show boxplots for each age group of the hospital admission dataset, from 2008 until 2019. The number of hospital admissions is similar for both genders, except between age groups 10-14 to 40-44 years old. By further analyzing the data, we see that this is driven by p*regnancy, childbirth and puerperium*, accounting for an overall of 60.8% of hospital admissions within these age groups for females.

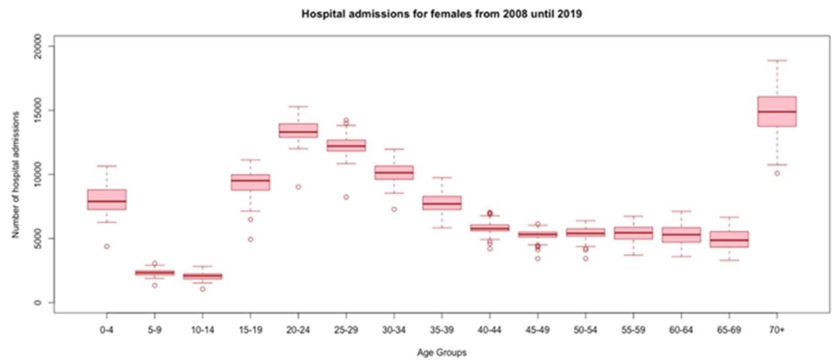


Figure 2. Hospital admissions of females by age group
Source: Authors, based on SIH/SUS data

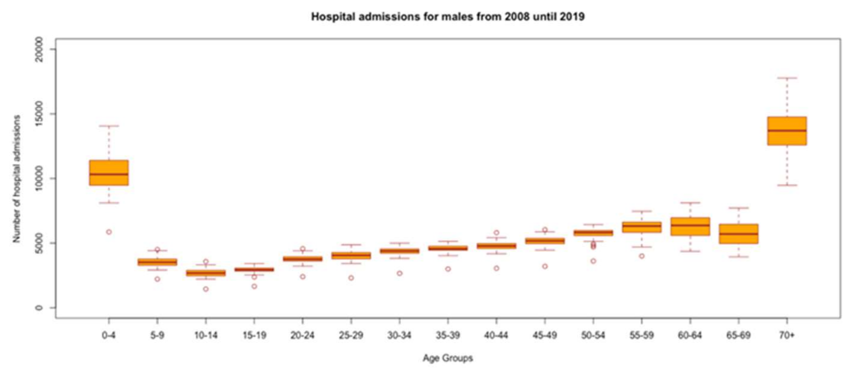


Figure 3. Hospital admissions of males by age groups
Source: Authors, based on SIH/SUS data

Figure 4 shows the female hospitalizations from Jan/2008 to Nov/2019 by age group. We see how the number of hospitalizations is distributed, with the age group 70+ being the highest in absolute number of hospitalizations. Similarly, Figure 5 shows the number of hospitalizations for males, also by age group. We can see that the age groups 0-4 years and 70+ years are the ones with the highest number of hospitalizations. In the other age groups, differently to what happens to females, the numbers of hospital admissions, by age group, are more similar.

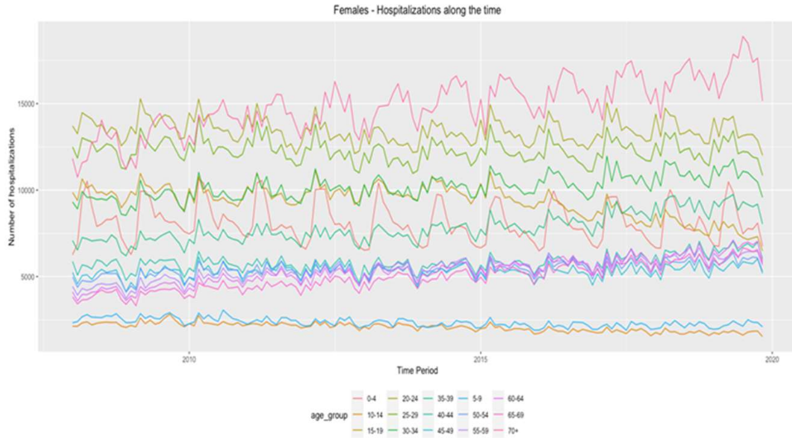


Figure 4. Female hospital admissions from Jan/2008 until Nov/2019
Source: Authors, based on SIH/SUS data

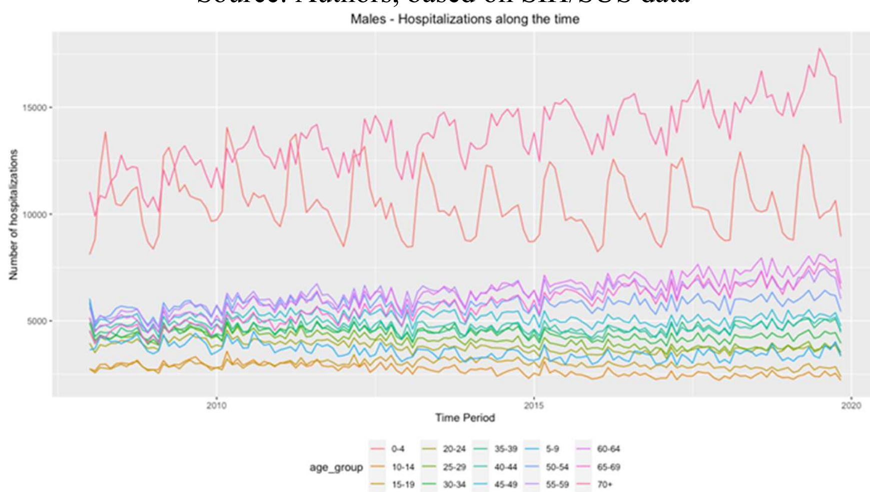


Figure 5. Male hospital admissions from Jan/2008 until Nov/2019
Source: Authors, based on SIH/SUS data

Figures 6 and 7 show the residents data, by age groups, for each gender. As shown in the charts, the distribution is similar for both sexes. Table 1 shows that there are generally more women than men, especially in the older age groups. This is due to the fact that women have a higher life expectancy than men.

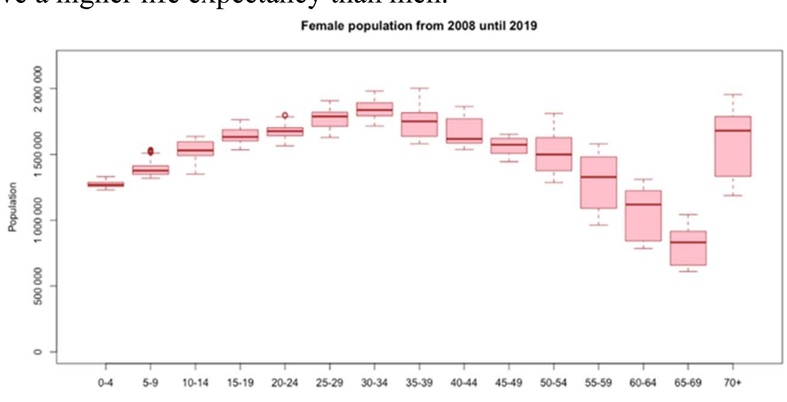


Figure 6. Female population by age groups
Source: Authors, based on PNAD/IBGE data

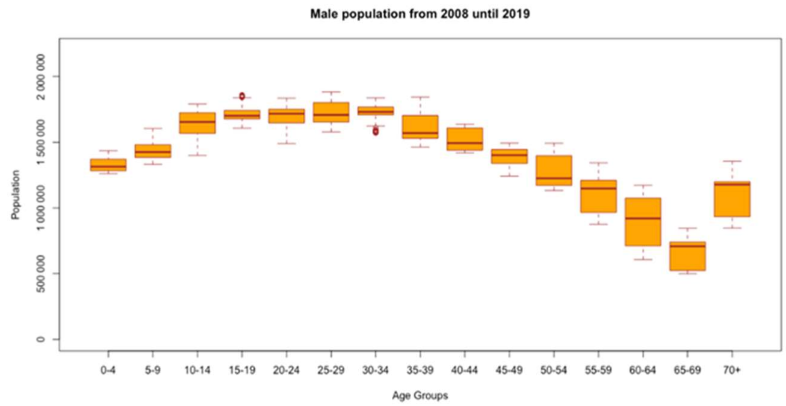


Figure 7. Male population by age groups
Source: Authors, based on PNAD/IBGE data

Table 1
Population distribution by gender

| Age Groups | Females | Males | Age Groups | Females | Males |
|---|---|---|---|---|---|
| 0-4 years | 49.0% | 51.0% | 40-44 years | 52.3% | 47.7% |
| 5-9 years | 49.2% | 50.8% | 45-49 years | 53.0% | 47.0% |
| 10-14 years | 48.8% | 51.2% | 50-54 years | 53.3% | 46.7% |
| 15-19 years | 49.3% | 50.7% | 55-59 years | 53.4% | 46.6% |
| 20-24 years | 49.9% | 50.1% | 60-64 years | 54.1% | 45.9% |
| 25-29 years | 51.2% | 48.8% | 65-69 years | 55.3% | 44.7% |
| 30-34 years | 51.7% | 48.3% | 70+ years | 59.2% | 40.8% |
| 35-39 years | 52.0% | 48.0% | Total | 51.6% | 48.4% |

Source: Authors, based on PNAD/IBGE data

## 3. Results and discussion

### 3.1 Results

In this work, we tested four learning rates and five decay values, for a total of 20 model combinations, per gender, to find the combination that minimizes the cost function. All models have the same structure, only the learning rate and the decay factor are varied. Table 2 shows the 20 alternatives.

Table 2
LSTM models

| Model | Learning rate | Decay Factor | Model | Learning rate | Decay Factor |
|---|---|---|---|---|---|
| Model 1 | 0.001 | 0 | Model 11 | 0.01 | 0 |
| Model 2 | 0.001 | 0.0000001 | Model 12 | 0.01 | 0.0000001 |
| Model 3 | 0.001 | 0.00001 | Model 13 | 0.01 | 0.00001 |
| Model 4 | 0.001 | 0.001 | Model 14 | 0.01 | 0.001 |
| Model 5 | 0.001 | 0.1 | Model 15 | 0.01 | 0.1 |
| Model 6 | 0.002 | 0 | Model 16 | 0.02 | 0 |
| Model 7 | 0.002 | 0.0000001 | Model 17 | 0.02 | 0.0000001 |
| Model 8 | 0.002 | 0.00001 | Model 18 | 0.02 | 0.00001 |
| Model 9 | 0.002 | 0.001 | Model 19 | 0.02 | 0.001 |
| Model 10 | 0.002 | 0.1 | Model 20 | 0.02 | 0.1 |

In the fitting step of the neural network, the model is iterated several times to adjust its parameters, in order to reduce the cost function. A training epoch refers to the number of passes of the entire training dataset through the neural network algorithm (Hastie et al., 2017, p. 397). The number of epochs can be determined using a graphic approach, by plotting the cost function in relation to the number of epochs. Figure 8 shows the Mean

Squared Error (MSE) cost function in relation to the number of epochs. We see that the error starts to rebound around the 25th epoch and that between the 20th and 25th epoch it did not considerably decrease. Given that, the number of 20 epochs was chosen to be used in this work.

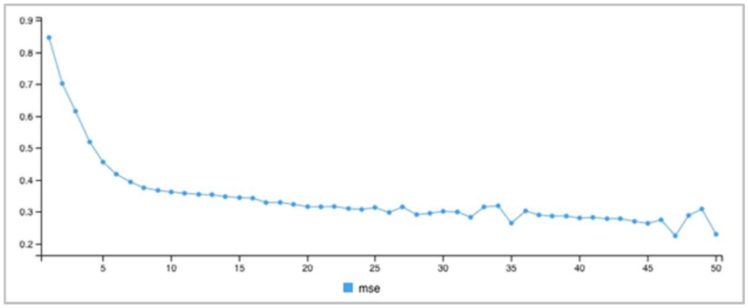


Figure 8. Cost function in relation to the number of epochs

Since the parameters of a neural network are randomly assigned, the backpropagation algorithm takes random weights and biases in order to minimize the cost function; each time the model is run it outputs a different result. Because of this stochastic behavior, to evaluate the model's performance it is necessary to ran it a sufficient number of times and calculate the average of the error metrics (Brownlee, 2017). A minimum number of 30 times is recommended by Brownlee (2017), limited only by computational resources and time expend running the model.

Given that a total of 20 model combinations have been explored, by varying the learning rate and a decay rate, it is worth to note that 30 random seeds were generated. This means that each round of each model was initialized with the same weights and biases so that any difference in performance can only be attributed to differences in the learning rate and decay. The LSTM models with the smallest average errors would be selected.

The process was developed for both genders, obtaining $k_t$ for males and females from 2008 to 2019. Figure 9 hows $k_t$ for both genders.

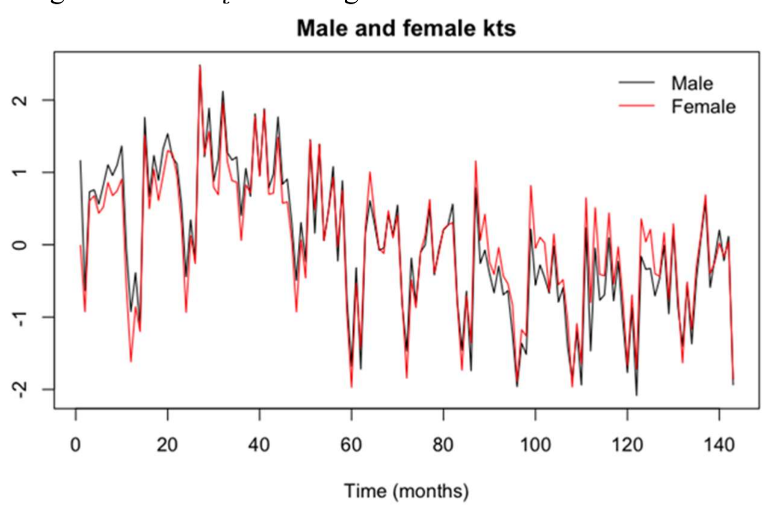


Figure 9. Males and females fitted $k_t$

~

The fitted $a_x$ and $b_x$ for each age group and gender are in Appendix (Table A1). In the prediction step, the next 12 months of $k_t$ were predicted. The *auto.arima* package chose the same $ARIMA(p, d, q)$ for both genders. This is not a surprise since both genders have similar trends, as shown in Figure 9. The mean and standard deviation of the training dataset calculated for standardizing purpose are in Table 3.

Table 3
Mean and standard deviation of females and males from training dataset

| Statistic | Female $k_t$ | Male $k_t$ |
|---|---|---|
| Mean | 0.09714466 | 0.1279912 |
| Standard Deviation | 0.91980280 | 0.9871962 |

The analysis of the results for the 20 alternatives leads to the conclusion that the LSTM models with the smallest average errors among the 20 models considered are Model 3 and Model 20, cf. Tables A2-A6 in the Appendix.
To evaluate the forecast performance of standard ARIMA versus LSTM Model 3 and LSTM Model 20, the Root Mean Squared Error (RMSE) and the Mean Absolute Error (MAE) error metrics were calculated. Table 4 summarizes the results.

Table 4
Comparing forecast performance between ARIMA and LSTM

| Model | Female | | Male | |
|---|---|---|---|---|
| | RMSE | MAE | RMSE | MAE |
| $k_t$ ARIMA | 0.4714 | 0.3452 | 0.4550 | 0.3655 |
| $k_t$ LSTM - Model 3 | 0.4974 | 0.4050 | 0.5635 | 0.4760 |
| $k_t$ LSTM - Model 20 | 0.4633 | 0.3582 | 0.5993 | 0.5059 |

The error in Model 3, for males, is higher than the error from the ARIMA model. For the females, in Model 20, only the RMSE is lower than the RMSE of the ARIMA model. Overall, both RMSE and MAE shown no great differences for females.
With these error metrics calculated, we have also performed the prediction of the next 12 months of $k_t$, for both genders, predicting how the $k_t$ would behave in the absence of the Covid-19 pandemic. The results are shown in Figures 10 and 11. We can see that the ARIMA and the LSTM models have similar patterns, which is not a surprise since the errors shown in Table 4 are similar.

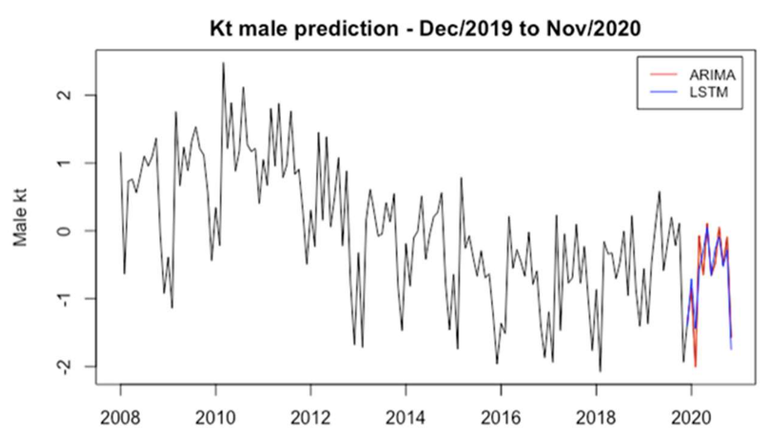

Figure 10. Male $k_t$ prediction for the next 12 months

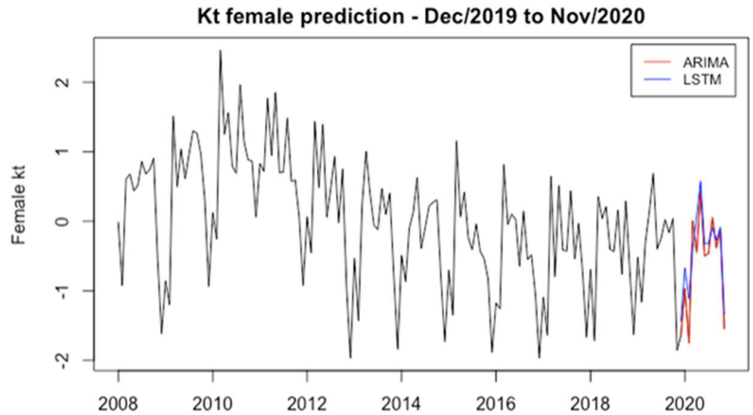

Figure 11. Female $k_t$ prediction for the next 12 months

## 3.2 Discussion

The main purpose of this work is to add a contribution to the set of applications of machine learning techniques in the actuarial science field, that has important socio economic responsibilities. The novelty is the application to model hospital admission rates using the LSTM neural network and to contrast its results with the results with the Lee-Carter model (Lee & Carter 1992), as done in Rodrigues et al. (2013). To the best of our knowledge, no analogous study has been done before.

With publicly available datasets about hospital admissions and population from the State of São Paulo, Brazil, a simple neural network architecture was implemented, and 20 LSTM models were built to search for the best combination of learning rates and decay factors, for each gender. Each of these 20 models was ran 30 times to average its RMSE and MAE results. This was performed in a personal computer, and it took around three hours, per each gender, to run. On the other hand, the *auto.arima* function took only a few seconds to find the best set of ARIMA parameters. The results for females provided by the neural network and by the ARIMA model were similar. For males, the ARIMA model performed better than the LSTM, showing lower RMSE and MAE. The results obtained are in line with Rodrigues et al. (2013), although not directly comparable. In their work they used annual data from the State of Minas Gerais, Brazil, while we used monthly data from the State of São Paulo, Brazil. The choice of using monthly data is to have more data points that can improve the estimates, while the choice of the State of São Paulo is because it is the largest state in Brazil, accounting for 22% of the Brazilian population (over 44 million), more than double the population of the State of Minas Gerais, which accounts for 10% of the population in the country (over 20 million) (IBGE, 2021).

In practical terms, by modeling hospital admission rates, actuaries can better assess the technical provisions of health insurance companies. In Brazil, there are the so-called *verticalized* health companies, which are health insurers that own hospitals and clinics in an attempt to control costs and frequency of use. For this type of company, modeling hospital admissions is even more important, as it not only allows them to more accurately determine their technical reserves, but also to better plan their human and medical resources, thereby improving their service to society.

Even though a small data sample was used in this work, the performances of the LSTM and ARIMA models were similar. It is well known that neural networks models demand huge amounts of data to be fitted but this similar performance suggests that future works with longer data sequences might cause LSTM modls to be better than the ARIMA approach.

## 4. Conclusion

The main objective of adding a contribution to the set of machine learning applications in actuarial science has been fully achieved. Further, our research has shown that, for the given problem and available data, the LSTM and ARIMA models perform similar in predicting the hospital admissions, which was not a disappointing outcome, on the contrary. From now, future works could rely on two approaches to test if the LSTM model can give a better outcome than the ARIMA: (i) work with longer data sequences. Comparing the ARIMA and LSTM on a daily sequence of data instead of a monthly one could show a significant difference in model performance; (ii) fine tune the LSTM model. Considering approach (ii), future work could explore the automatic search of parameters to adjust the neural network, but researchers and practitioners should be aware that it can be computational costly. The work of (Jin et al., 2019) proposed the package *AutoKeras* for this search, implemented in Python, which they claim to be efficient when compared to existing auto-search algorithms. The use of regularization techniques in neural networks should also be explored, see (Hastie et al., 2017; Chollet, 2018). This gives a possibility to improve results and to study how the use of different regularization techniques impacts on the performance of neural networks.

Despite the much greater time required to prepare the data and to effectively run the neural network model, any action that can help to ensure the solvency of insurance companies in a line of business with such a social impact as health insurance is worthwhile and highly valuable.


## Acknowledgements

The authors acknowledge financial support from FCT – Fundação para a Ciência e Tecnologia (Portugal), national funding through research grant UIDB/05069/2020.


## References


Abadi, M. (2015). TensorFlow: Large-scale machine learning on heterogeneous systems. https://www.tensorflow.org .

Bengio, Y. (2012). Pratical Recommendations for Gradient-Based Training of Deep Architectures. In *Neural Networks: Tricks of the Trade* (2nd edition, pp. 437-478). Berlin, Heidelberg: Springer.

Brownlee, J. (2017). *Long Short-Term Memory Networks With Python: Develop Sequence Prediction Models With Deep Learning.* Machine Learning Mastery.

Brownlee, J. (2018). *Deep Learning for Time Series Forecasting - Predict the Future with MLPs, CNNs and LSTMs in Python.* Machine Learning Mastery.

Cechin, J. & Lara, N. (2020). *Análise Especial do Mapa Assistencial da Saúde Suplementar no Brasil Entre 2014 e 2019.* São Paulo: Instituto de Estudos da Saúde Suplementar. https://www.iess.org.br/biblioteca/tds-e-estudos/estudos-especiais-do-iess/analise-especial-do-mapa-assistencial-da-saude

Chollet, F. (2015). Keras. https://keras.io .

Chollet, F. (2018). *Deep Learning with Python.* United States of America: Manning Publications Co.

Deaton, A. & Paxson, C. (2004). *Mortality, Income and Income Inequality Over Time in the Britain and the United States.* In *Perspectives on the Economics of Aging (pp. 247-286).* National Bureau of Economic Research, Inc.

Deprez, P., Shevchenko, P. V. & Wüthrich, M. V. (2017). Machine Learning Techniques for Mortality Modeling. *European Actuarial Journal, 7*, 337-352. https://doi.org/10.1007/s13385-017-0152-4

Dong, X., Kedziora, D. J., Musial, K. & Gabrys, B. (2021). Automated Deep Learning: Neural Architecture Search Is Not the End. *arXiv.* https://doi.org/10.48550/arxiv.2112.09245

European Commission, Directorate-General for Economic and Financial Affairs, Schwierz, C., Medeiros, J. (2013). *Estimating the drivers and projecting long-term public health expenditure in the European Union: Baumol's «cost disease» revisited*, European Commission. https://data.europa.eu/doi/10.2765/54565

Frees, E. (2006). Forecasting labor force participation rates. *Journal of Official Statistics, 22*(3), 453-485.

Gers, F., Schmidhuber, J. & Cummins, F. (2000). Learning to forget: Continual prediction with LSTM. *Neural Computation, 12*(10), 2451-2471. https://doi.org/10.1162/089976600300015015

Girosi, F. & King, G. (2008). *Demographic Forecasting.* Princeton University Press.

Goodfellow, I., Bengio, Y. & Courville, A. (2016). *Deep Learning.* MIT Press.

Gutterman, S. & Vanderhoof, I. T. (1998). Forecasting changes in mortality: a search for a law of causes and effects. *North American Actuarial Journal, 2*(4), 135-138.

Hainaut, D. (2018). A Neural-Network Analyzer for Mortality Forecast. *ASTIN Bulletin, 48*(2), 481-508. https://doi.org/10.1017/asb.2017.45

Hastie, T., Tibshirani, R. & Friedman, J. (2017). *The Elements of Statistical Learning: Data Mining, Inference, and Prediction* (2nd Edition). Springer.

Heaton, J. (2005). *Introduction to Neural Networks with Java* (1st Edition). Heaton Research.

Hochreiter, S. & Schmidhuber, J. (1997). Long Short-Term Memory. *Neural Computation, 9*(8), 1735-1780. https://doi.org/10.1162/neco.1997.9.8.1735

Hollmann, F. W., Mulder, T. J. & Kallan, J. E. (2000). *Methodology and Assumptions for the Population Projections of the United States: 1999 to 2100.* (Working Paper No. POP-WP038), U.S. Bureau of Census, Population Division.

Hu, X., Chu, L., Pei, J., Liu, W. & Bian, J. (2021). Model Complexity of Deep Learning: A Survey. *Knowledge and Information Systems, 63*, 2585-2619. https://doi.org/10.1007/s10115-021-01605-0

Hyndman, R., Athanasopoulos, G., Bergmeir, C., Caceres, G., Chhay, L., O'Hara-Wild M., … Yasmeen F. (2022). forecast: Forecasting Functions for Time Series and Linear Models. R package version 8.16, URL: https://pkg.robjhyndman.com/forecast/

Hyndman, R. J. & Khandakar, Y. (2008). Automatic time series forecasting: the forecast package for R. *Journal of Statistical Software, 26*(3), 1–22. https://doi.org/10.18637/jss.v027.i03

IBGE. Instituto Brasileiro de Geografia e Estatística (2021). Estimativas da População Residente no Brasil e Unidades da Federação com data de Referência em 1 de Julho de 2021. Retrieved from https://biblioteca.ibge.gov.br/visualizacao/livros/liv101849.pdf

Jin, H., Song, Q. & Hu, X. (2019). Auto-Keras: An Efficient Neural Architecture Search System. *arXiv*. https://doi.org/10.48550/arXiv.1806.10282

Kjærgaard, S. & Bergeron-Boucher, M.-P. (2022). Mortality forecasting at age 65 and above: an age-specific evaluation of the Lee-Carter model. *Scandinavian Actuarial Journal*, *1*, 64-79. https://doi.org/10.1080/03461238.2021.1928542

Lee, R. & Carter, L. (1992). Modeling and Forecasting US Mortality. *Journal of the American Statistical Association, 87*, 659–671. https://doi.org/10.2307/2290201

Lee, R. & Miller, T. (2002). An Apporach to Forecasting Health Expenditures with Application to the U.S. Medicare System. *Health Services Research (Ann Arbor), 37*(5), 1365-1386. https://doi.org/10.1111/1475-6773.01112

Levantesi, S. & Pizzorusso, V. (2019). Application of machine learning to mortality modeling and forecasting. *Risks, 7*(1), 26. https://doi.org/10.3390/risks7010026

Lindberg, C. & McCarthy, T. (2021). Impact of Demographic Change on Health Expenditure 2022-2025. Report prepared by the Irish Government Economic and Evaluation Service (IGEES) staff in the Department of Health.

McCulloch, W. S. & Pitts, W. (1943). A logical calculus of the ideas immanent in nervous activity. *Bulletin of Mathematical Biophysics, 5*, 115–133. https://doi.org/10.1007/BF02478259

Minsky, M. & Seymour, P. (2017). *Perceptrons, Reissue of the 1988 Expanded Edition with a new Foreword by Léon Bottou.* Cambridge: Massachusetts Institute of Technology Press.

Namini, S. & Namin, A. (2018). Forecasting Economic and Financial Time Series: ARIMA vs. LSTM. *ArXiv.* https://doi.org/10.48550/arXiv.1803.06386

Nigri, A., Levantesi, S. & Marino, M. (2021). Life expetancy and lifespan disparity forecasting: a long short-term memory approach. *Scandinavian Actuarial Journal 2021, 2*, 110-133. https://doi.org/10.1080/03461238.2020.1814855

Nigri, A., Levantesi, S., Marino, M., Scognamiglio, S., & Perla, F. (2019). A Deep Learning Integrated Lee–Carter Model. *Risks, 7*(1), 33. https://doi.org/10.3390/risks7010033

Perla, F., Richman, R., Scognamiglio, S. & Wüthrich, M. (2021). Time-series forecasting of mortality rates using deep learning. *Scandinavian Actuarial Journal 2021*, *7*, 572-598. https://doi.org/10.1080/03461238.2020.1867232

Rabbi, A. & Mazzuco, S. (2020). Mortality Forecasting with the Lee–Carter Method: Adjusting for Smoothing and Lifespan Disparity. *European Journal of Population, 37*(1), 97-120. https://doi.org/10.1007/s10680-020-09559-9

Richman, R. & Wüthrich, M. V. (2018). A Neural Network Extension of the Lee-Carter Model to Multiple Populations. http://dx.doi.org/10.2139/ssrn.3270877

Rodrigues, C. G., Andrade, M. V., Queiroz, B. L. & Machado, C. J. (2013). *The Applicability of the Lee-Carter Method to Forecast Health Services Use in Brazil.* In: Hoque, N., McGehee, M., Bradshaw, B. (eds) Applied Demography and Public Health. Applied Demography Series, vol 3. Springer, Dordrecht. https://doi.org/10.1007/978-94-007-6140-7_21

Steeghs, K. (2020). Parameter Uncertainty in the Lee-Carter Model. *Network for Studies on Pensions, Aging and Retirement* (Master's thesis, Maastricht University, Amsterdam, The Netherlands). Retrieved from https://www.netspar.nl/assets/uploads/P20200814_MSc014_Steeghs.pdf

Tate, R. B., MacWilliam, L. R. & Finlayson, G. (2005). A Methodology for Evaluating Hospital Bed Need in Manitoba in 2020. *Canadian Journal on Aging/La Revue canadienne du vieillissement, 24*(5), 141-151. https://doi.org/10.1353/cja.2005.0056

Tuljapurkar, S., Li, N. & Boe, C. (2000). A universal pattern of mortality decline in the G7 countries. *Nature 405*, 789-792. https://doi.org/10.1038/35015561

United Nations. (1952). *Methods of Estimating Total Population for Current Dates.*

Uzair, M. & Jamil, N. (2020). Effects of Hidden Layers on the Efficiency of Neural networks. *2020 IEEE 23rd International Multitopic Conference (INMIC)*, 1-6. https://doi.org/10.1109/INMIC50486.2020.9318195

Wang, J., You, K., Long, M. & Jordan, M. I. (2019). How Does Learning Rate Decay Help Modern Neural Networks? *arXiv*. https://doi.org/10.48550/arXiv.1908.01878

Wiener, N. (1948). *Cybernetics: Or Control and Communication in the Animal and the Machine,* (2nd ed.). Cambridge: Massachusetts Institute of Technology Press.

Wilmoth. (1996). Mortality projections for Japan. In: *Health and mortality among elderly populations* (pp. 266-288). Clarendon Press.

Xu, K., Saksena, P. & Holly, A. (2011). The determinants of health expenditure. A country-level panel data analysis. *(WHO Working Paper R4D). Geneva: World Health Organization*.

Appendix

Table A1

Fitted $a_x$ and $b_x$ for females and males, by age group

| Age Group | Females | | Males | |
|---|---|---|---|---|
| | $a_x$ | $b_x$ | $a_x$ | $b_x$ |
| 0-4 | -5.065297 | 0.10449056 | -4.845265 | 0.08736755 |
| 5-9 | -6.391685 | 0.07711722 | -6.002098 | 0.06256431 |
| 10-14 | -6.613553 | 0.07728216 | -6.405589 | 0.05413556 |
| 15-19 | -5.176530 | 0.06819218 | -6.368512 | 0.04540376 |
| 20-24 | -4.826560 | 0.02003936 | -6.106506 | 0.03171212 |
| 25-29 | -4.974457 | 0.02094504 | -6.049290 | 0.04420463 |
| 30-34 | -5.197766 | 0.02922902 | -5.972261 | 0.06880108 |
| 35-39 | -5.416896 | 0.04026236 | -5.862534 | 0.07340256 |
| 40-44 | -5.656251 | 0.06463627 | -5.762601 | 0.08326992 |
| 45-49 | -5.690644 | 0.07470302 | -5.599314 | 0.06810099 |
| 50-54 | -5.621203 | 0.08955646 | 5.397862 | 0.07876780 |
| 55-59 | -5.479867 | 0.08348134 | -5.181277 | 0.06963178 |
| 60-64 | -5.301539 | 0.08582828 | -4.965034 | 0.08479263 |
| 65-69 | -5.091800 | 0.07347616 | -4.740753 | 0.06855017 |
| 70+ | -4.668532 | 0.09076058 | -4.391226 | 0.07929514 |

Table A2

Model summary - Females and Males

```
Model: "sequential"
_________________________________________________________________
 Layer (type)                    Output Shape              Param #
=================================================================
 LSTM (LSTM)                     (1, 12, 12)               672
 Output (TimeDistributed)        (1, 12, 1)                13
=================================================================
Total params: 685
Trainable params: 685
Non-trainable params: 0
_________________________________________________________________
```

Table A3

Female LSTM - RMSE metrics

| Model | Learning Rate | decay | avg_rmse | sd_rmse | min_rmse | q25_rmse | median_rmse | q75_rmse | max_rmse |
|---|---|---|---|---|---|---|---|---|---|
| Model 1 | 0,001 | 0 | 0,4978 | 0,0107 | 0,4763 | 0,489675 | 0,49785 | 0,506725 | 0,519 |
| Model 2 | 0,001 | 1,00E-07 | 0,498 | 0,0109 | 0,4762 | 0,48985 | 0,4977 | 0,50845 | 0,5184 |
| Model 3 | 0,001 | 1,00E-05 | 0,4974 | 0,0105 | 0,4769 | 0,4903 | 0,4974 | 0,506775 | 0,5165 |
| Model 4 | 0,001 | 0,001 | 0,4912 | 0,0079 | 0,4789 | 0,4859 | 0,4898 | 0,497125 | 0,5141 |
| Model 5 | 0,001 | 0,1 | 0,7828 | 0,0661 | 0,6774 | 0,732475 | 0,76195 | 0,845375 | 0,8936 |
| Model 6 | 0,002 | 0 | 0,504 | 0,0141 | 0,476 | 0,495475 | 0,50475 | 0,511175 | 0,5406 |
| Model 7 | 0,002 | 1,00E-07 | 0,504 | 0,0147 | 0,4764 | 0,495025 | 0,5035 | 0,511525 | 0,5406 |
| Model 8 | 0,002 | 1,00E-05 | 0,5049 | 0,0126 | 0,482 | 0,496625 | 0,5045 | 0,511275 | 0,5348 |
| Model 9 | 0,002 | 0,001 | 0,499 | 0,0114 | 0,4759 | 0,491975 | 0,49765 | 0,50725 | 0,5208 |
| Model 10 | 0,002 | 0,1 | 0,7241 | 0,0515 | 0,6355 | 0,68995 | 0,7158 | 0,770375 | 0,8149 |
| Model 11 | 0,01 | 0 | 0,4938 | 0,0326 | 0,4286 | 0,469725 | 0,4881 | 0,5106 | 0,5883 |
| Model 12 | 0,01 | 1,00E-07 | 0,4889 | 0,0303 | 0,4443 | 0,468775 | 0,48315 | 0,50165 | 0,5615 |
| Model 13 | 0,01 | 1,00E-05 | 0,4931 | 0,0306 | 0,4296 | 0,478625 | 0,4861 | 0,5148 | 0,5459 |
| Model 14 | 0,01 | 0,001 | 0,5032 | 0,0313 | 0,4365 | 0,48515 | 0,50505 | 0,5178 | 0,5938 |
| Model 15 | 0,01 | 0,1 | 0,4881 | 0,0238 | 0,4534 | 0,466725 | 0,49025 | 0,50035 | 0,5343 |
| Model 16 | 0,02 | 0 | 0,5062 | 0,033 | 0,4468 | 0,4806 | 0,5091 | 0,523025 | 0,5698 |
| Model 17 | 0,02 | 1,00E-07 | 0,5014 | 0,0291 | 0,4549 | 0,4772 | 0,49835 | 0,520075 | 0,5841 |
| Model 18 | 0,02 | 1,00E-05 | 0,5058 | 0,0252 | 0,455 | 0,488175 | 0,50685 | 0,51765 | 0,5525 |
| Model 19 | 0,02 | 0,001 | 0,4805 | 0,0268 | 0,4381 | 0,4651 | 0,4836 | 0,49875 | 0,5461 |
| Model 20 | 0,02 | 0,1 | 0,4633 | 0,0076 | 0,4483 | 0,459825 | 0,46365 | 0,4666 | 0,4778 |

Table A4
Female LSTM - MAE metrics

| Model | Learning Rate | decay | avg_mae | sd_mae | min_mae | q25_mae | median_mae | q75_mae | max_mae |
|---|---|---|---|---|---|---|---|---|---|
| Model 1 | 0,001 | 0 | 0,4049 | 0,0165 | 0,379 | 0,387175 | 0,40655 | 0,41555 | 0,4355 |
| Model 2 | 0,001 | 1,00E-07 | 0,4054 | 0,0163 | 0,3785 | 0,39345 | 0,40575 | 0,416225 | 0,4354 |
| Model 3 | 0,001 | 1,00E-05 | 0,405 | 0,0156 | 0,3803 | 0,39005 | 0,407 | 0,4157 | 0,4348 |
| Model 4 | 0,001 | 0,001 | 0,3967 | 0,0118 | 0,3735 | 0,38685 | 0,39675 | 0,40565 | 0,4229 |
| Model 5 | 0,001 | 0,1 | 0,5407 | 0,0596 | 0,4425 | 0,492925 | 0,52625 | 0,593 | 0,6406 |
| Model 6 | 0,002 | 0 | 0,4097 | 0,0151 | 0,3797 | 0,400525 | 0,4079 | 0,42205 | 0,4437 |
| Model 7 | 0,002 | 1,00E-07 | 0,4093 | 0,0174 | 0,3652 | 0,397675 | 0,4109 | 0,420075 | 0,4437 |
| Model 8 | 0,002 | 1,00E-05 | 0,4111 | 0,0141 | 0,3802 | 0,401325 | 0,4123 | 0,42065 | 0,4378 |
| Model 9 | 0,002 | 0,001 | 0,401 | 0,0141 | 0,3765 | 0,39175 | 0,39845 | 0,413975 | 0,4239 |
| Model 10 | 0,002 | 0,1 | 0,4942 | 0,0423 | 0,4165 | 0,4672 | 0,48575 | 0,52735 | 0,5705 |
| Model 11 | 0,01 | 0 | 0,3824 | 0,0361 | 0,3046 | 0,3596 | 0,37575 | 0,40485 | 0,4594 |
| Model 12 | 0,01 | 1,00E-07 | 0,3828 | 0,0382 | 0,3339 | 0,3549 | 0,3745 | 0,404425 | 0,4829 |
| Model 13 | 0,01 | 1,00E-05 | 0,3836 | 0,0318 | 0,3394 | 0,365225 | 0,3741 | 0,401525 | 0,4775 |
| Model 14 | 0,01 | 0,001 | 0,3967 | 0,0299 | 0,3346 | 0,374575 | 0,3931 | 0,409525 | 0,4696 |
| Model 15 | 0,01 | 0,1 | 0,3627 | 0,0285 | 0,3139 | 0,342 | 0,3648 | 0,3766 | 0,4262 |
| Model 16 | 0,02 | 0 | 0,3937 | 0,0359 | 0,3114 | 0,370075 | 0,39035 | 0,41935 | 0,459 |
| Model 17 | 0,02 | 1,00E-07 | 0,3915 | 0,0333 | 0,3269 | 0,36835 | 0,39445 | 0,412275 | 0,4718 |
| Model 18 | 0,02 | 1,00E-05 | 0,3968 | 0,033 | 0,3304 | 0,3762 | 0,39895 | 0,4135 | 0,4733 |
| Model 19 | 0,02 | 0,001 | 0,3813 | 0,0351 | 0,3046 | 0,3698 | 0,3828 | 0,409475 | 0,4643 |
| Model 20 | 0,02 | 0,1 | 0,3582 | 0,0102 | 0,3351 | 0,350725 | 0,3576 | 0,365175 | 0,3785 |

Table A5
Male LSTM - RMSE metrics

| Model | Learning Rate | decay | avg_rmse | sd_rmse | min_rmse | q25_rmse | median_rmse | q75_rmse | max_rmse |
|---|---|---|---|---|---|---|---|---|---|
| Model 1 | 0,001 | 0 | 0,5643 | 0,0162 | 0,5285 | 0,54935 | 0,5682 | 0,577725 | 0,5873 |
| Model 2 | 0,001 | 1,00E-07 | 0,5641 | 0,0155 | 0,5357 | 0,5493 | 0,56655 | 0,57765 | 0,5867 |
| Model 3 | 0,001 | 1,00E-05 | 0,5635 | 0,0165 | 0,5305 | 0,549325 | 0,56285 | 0,577975 | 0,5908 |
| Model 4 | 0,001 | 0,001 | 0,5878 | 0,024 | 0,5376 | 0,571475 | 0,58625 | 0,609325 | 0,6273 |
| Model 5 | 0,001 | 0,1 | 0,7715 | 0,068 | 0,6747 | 0,717675 | 0,74615 | 0,826325 | 0,9021 |
| Model 6 | 0,002 | 0 | 0,5876 | 0,026 | 0,5416 | 0,570275 | 0,58885 | 0,599975 | 0,6482 |
| Model 7 | 0,002 | 1,00E-07 | 0,5895 | 0,0265 | 0,5433 | 0,5698 | 0,58685 | 0,60265 | 0,6483 |
| Model 8 | 0,002 | 1,00E-05 | 0,5926 | 0,0324 | 0,5387 | 0,568475 | 0,58875 | 0,610125 | 0,6713 |
| Model 9 | 0,002 | 0,001 | 0,5719 | 0,0187 | 0,5398 | 0,5607 | 0,573 | 0,580925 | 0,6123 |
| Model 10 | 0,002 | 0,1 | 0,7311 | 0,0268 | 0,6868 | 0,70915 | 0,7346 | 0,74895 | 0,7969 |
| Model 11 | 0,01 | 0 | 0,5897 | 0,0368 | 0,532 | 0,5673 | 0,5816 | 0,603 | 0,6823 |
| Model 12 | 0,01 | 1,00E-07 | 0,5899 | 0,042 | 0,517 | 0,565425 | 0,58575 | 0,60205 | 0,6987 |
| Model 13 | 0,01 | 1,00E-05 | 0,5877 | 0,043 | 0,4873 | 0,5575 | 0,58365 | 0,623475 | 0,6689 |
| Model 14 | 0,01 | 0,001 | 0,6075 | 0,0302 | 0,5542 | 0,58465 | 0,6065 | 0,627275 | 0,6945 |
| Model 15 | 0,01 | 0,1 | 0,7165 | 0,0339 | 0,6301 | 0,6879 | 0,7207 | 0,743525 | 0,7759 |
| Model 16 | 0,02 | 0 | 0,5987 | 0,0774 | 0,4884 | 0,550875 | 0,59505 | 0,626975 | 0,8794 |
| Model 17 | 0,02 | 1,00E-07 | 0,616 | 0,081 | 0,4951 | 0,5749 | 0,60305 | 0,632825 | 0,9174 |
| Model 18 | 0,02 | 1,00E-05 | 0,6056 | 0,0566 | 0,4518 | 0,57455 | 0,6051 | 0,63895 | 0,7048 |
| Model 19 | 0,02 | 0,001 | 0,6125 | 0,0502 | 0,5284 | 0,579825 | 0,60875 | 0,641975 | 0,7262 |
| Model 20 | 0,02 | 0,1 | 0,5993 | 0,0182 | 0,5702 | 0,58855 | 0,599 | 0,60615 | 0,6576 |

Table A6
Male LSTM - MAE metrics

| Model | Learning Rate | decay | avg_mae | sd_mae | min_mae | q25_mae | median_mae | q75_mae | max_mae |
|---|---|---|---|---|---|---|---|---|---|
| Model 1 | 0,001 | 0 | 0,4768 | 0,0194 | 0,4399 | 0,4604 | 0,4818 | 0,492625 | 0,5051 |
| Model 2 | 0,001 | 1,00E-07 | 0,4769 | 0,0183 | 0,4399 | 0,46375 | 0,48095 | 0,489975 | 0,505 |
| Model 3 | 0,001 | 1,00E-05 | 0,476 | 0,0191 | 0,4449 | 0,4606 | 0,4789 | 0,4913 | 0,5112 |
| Model 4 | 0,001 | 0,001 | 0,4976 | 0,0275 | 0,4396 | 0,479825 | 0,4917 | 0,520975 | 0,5406 |
| Model 5 | 0,001 | 0,1 | 0,5836 | 0,0461 | 0,5049 | 0,5521 | 0,5748 | 0,6186 | 0,6716 |
| Model 6 | 0,002 | 0 | 0,5014 | 0,0256 | 0,4504 | 0,485425 | 0,50105 | 0,517725 | 0,5574 |
| Model 7 | 0,002 | 1,00E-07 | 0,5028 | 0,0247 | 0,4593 | 0,483275 | 0,50045 | 0,520425 | 0,5576 |
| Model 8 | 0,002 | 1,00E-05 | 0,5062 | 0,0312 | 0,4485 | 0,481825 | 0,50905 | 0,5276 | 0,5674 |
| Model 9 | 0,002 | 0,001 | 0,4849 | 0,0222 | 0,4428 | 0,46945 | 0,4866 | 0,497275 | 0,5322 |
| Model 10 | 0,002 | 0,1 | 0,5904 | 0,0327 | 0,5296 | 0,570925 | 0,5905 | 0,61305 | 0,6616 |
| Model 11 | 0,01 | 0 | 0,4971 | 0,0403 | 0,4258 | 0,47655 | 0,4917 | 0,512 | 0,591 |
| Model 12 | 0,01 | 1,00E-07 | 0,502 | 0,0396 | 0,4209 | 0,477675 | 0,50455 | 0,522875 | 0,5932 |
| Model 13 | 0,01 | 1,00E-05 | 0,4963 | 0,0534 | 0,3824 | 0,465875 | 0,4992 | 0,5468 | 0,5794 |
| Model 14 | 0,01 | 0,001 | 0,5158 | 0,0318 | 0,4656 | 0,4936 | 0,51355 | 0,537675 | 0,598 |
| Model 15 | 0,01 | 0,1 | 0,6172 | 0,0357 | 0,54 | 0,58625 | 0,6182 | 0,6479 | 0,6775 |
| Model 16 | 0,02 | 0 | 0,5044 | 0,0744 | 0,382 | 0,463425 | 0,4994 | 0,539575 | 0,791 |
| Model 17 | 0,02 | 1,00E-07 | 0,5197 | 0,0817 | 0,3966 | 0,4806 | 0,51295 | 0,546075 | 0,8468 |
| Model 18 | 0,02 | 1,00E-05 | 0,5106 | 0,0565 | 0,3752 | 0,4745 | 0,51595 | 0,550625 | 0,6077 |
| Model 19 | 0,02 | 0,001 | 0,5236 | 0,0514 | 0,4215 | 0,488925 | 0,5193 | 0,5606 | 0,6513 |
| Model 20 | 0,02 | 0,1 | 0,5059 | 0,0241 | 0,462 | 0,49285 | 0,5056 | 0,51935 | 0,579 |